Theoretical Study of Internal Conversion Decay Rates Associated with the Three Lowest Singlet Electronic States in Pyrazine

Reza Islampour* and Mahsa Miralinaghi

Department of Chemistry, Tarbiat Moallem University, 49 Mofateh Avenue, Tehran, Iran

Received: August 13, 2008; Revised Manuscript Received: November 4, 2008

The general expressions we recently derived for calculating internal conversion decay rate constants between two adiabatic and between two diabatic displaced−distorted−rotated harmonic potential energy surfaces (including all vibrational modes) are now applied to determine the decay rate constants of $^1B_{2u}(\pi\pi^*)\rightarrow{}^1B_{3u}(n\pi^*)$, $^1B_{2u}(\pi\pi^*)\rightarrow{}^1A_g$, and $^1B_{3u}(n\pi^*)\rightarrow{}^1A_g$ internal conversions in pyrazine molecule. The minimal models with respect to the number and the types of vibrational modes are investigated for these processes. An exact expression for the adiabatic vibrational frequencies of the coupling modes in terms of interstate coupling constants and the parameters determining the diabatic potential energy surfaces are also derived.

1. Introduction

Pyrazine has two close-lying lowest singlet excited electronic states $^1B_{3u}(n\pi^*)$ and $^1B_{2u}(\pi\pi^*)$. The electronic absorption spectra from the ground electronic state ^1A_g to the excited electronic states $^1B_{3u}$ and $^1B_{2u}$ have been widely studied.[1−5] The $n\pi^*$ absorption exhibits well-resolved band system, while the $\pi\pi^*$ excitation results in a broadband system with little structure that indicates an ultrafast (on a femtosecond time scale) $^1B_{2u}\rightarrow{}^1B_{3u}$ internal conversion process. As a result, $^1A_g\rightarrow{}^1B_{3u}$ excitation has been almost completely analyzed, but much of the photophysical dynamics of the $^1B_{3u}$ is still under investigation. In addition, the molecule exhibits fluorescence with a low quantum yield both in solution[6] and in the vapor,[7] but strong phosphorescence in the vapor and condensed phases.[8,9]

The unusual electronic absorption and the ultrafast electronic relaxation are ascribed to the (linear) vibronic coupling between $^1B_{3u}$ and $^1B_{2u}$ excited electronic states through the mode ν_{10a} of symmetry b_{1g}, which is the only mode of this species in the molecule.[4] The coupling is strong enough to cause the distortion of potential energy surfaces along this mode and ν_{10a} progressions to appear in absorption and fluorescence spectra with anomalous anharmonic level spacing in $^1B_{3u}$ and (perhaps) $^1B_{2u}$ manifold.[2,4]

Theoretical efforts have been made to simulate the $^1B_{3u}$ and $^1B_{2u}$ absorption (as well as resonance Raman) spectra and the ultrafast $^1B_{2u}\rightarrow{}^1B_{3u}$ electronic relaxation. To that end, several model Hamiltonians of increasing dimensionality and complexity in the diabatic electronic representation have been employed. The models that differ in the expansion orders for the diagonal and off-diagonal matrix elements of the Hamiltonian matrix and the number of the vibrational modes taken into account are called the 4-mode model,[10] 7-mode model,[11] 24-mode system-bath model,[12−15] and 24-mode pyrazine model.[16,17] The last model is the most realistic model in which the correct symmetry of all 24 modes of the pyrazine molecule is considered. The calculations based on these model Hamiltonians reproduce the essential features of $^1B_{3u}$ and $^1B_{2u}$ absorption (and resonance Raman[11]) spectra; however, to simulate the broad spectral envelope of the $^1B_{2u}$, a phenomenological broadening has to be taken into the calculations. Besides, the ultrafast electronic relaxation decay can be inferred from these models.[14,17,23,34,35]

It has been experimentally found that the $^1B_{3u}\rightarrow{}^1A_g$ internal conversion decay time constant varies from about 10 ns for the ground vibrational state[19] to (22 ± 1) ps for highly excited vibrational states[18−21] of the $^1B_{3u}$ excited electronic state. Accordingly, the decay time constant of $^1B_{2u}\rightarrow{}^1B_{3u}$ internal conversion is (20 ± 10) fs,[21] and that of $^1B_{2u}\rightarrow{}^1A_g$ internal conversion is about 13 ps (estimated from Figure 5 of ref19) for the ground vibrational state of the $^1B_{2u}$ excited electronic state.

It is the purpose of this Article to calculate the internal conversion decay rate constants associated with the three lowest singlet electronic states $^1B_{2u}$, $^1B_{3u}$, and ^1A_g in pyrazine molecule. The general expressions recently derived[22] for the decay rate constants between two adiabatic and between two diabatic displaced−distorted−rotated harmonic potential energy surfaces, including all vibrational modes, are employed. Calculation of rate constants involving the adiabatic potential surfaces requires the adiabatic vibrational frequencies, so a general exact expression for the adiabatic frequencies in terms of the coupling constants and the parameters determining the diabatic potential surfaces is derived in advance.

2. Theory

2.1. Vibronic Hamiltonian Matrix. The vibronic states of a molecular system can be described in the adiabatic or diabatic electronic representation.[25,26]

In the adiabatic electronic representation, the electronic states $\{\Phi_n(\mathbf{r},\mathbf{Q})\}$ are defined as the eigenstates of the electronic Hamiltonian:

$$[\hat{T}_e(\mathbf{r}) + \hat{U}(\mathbf{r},\mathbf{Q})]|\Phi_n\rangle = E_n(\mathbf{Q})|\Phi_n\rangle \qquad (1)$$

where $\hat{T}_e(\mathbf{r})$ is the electronic kinetic energy and $\hat{U}(\mathbf{r},\mathbf{Q})$ is the total potential energy operator. The exact vibronic states are then expanded in the adiabatic electronic states as:

$$|\psi_j\rangle = \sum_n \chi_n^{(j)}(\mathbf{Q})|\Phi_n\rangle \qquad (2)$$

and the expansion coefficients $\chi_n^{(j)}(\mathbf{Q})$ are determined by substitution of this expansion in the Schrodinger equation:

* Corresponding author. E-mail: islampour@saba.tmu.ac.ir.

10.1021/jp8072206 CCC: $40.75
Published on Web 02/11/2009

$$[\hat{T}_e(\mathbf{r}) + \hat{T}_N(\mathbf{Q}) + \hat{U}(\mathbf{r},\mathbf{Q})]|\psi_j\rangle = \varepsilon_j|\psi_j\rangle \quad (3)$$

where $\hat{T}_N(\mathbf{Q})$ is the nuclear kinetic energy operator. However, this leads to a coupled set of nonlinear equations. To linearize these equations, we expand the adiabatic coefficients $\chi_n^{(j)}(\mathbf{Q})$ for each adiabatic electronic state $|\Phi_n\rangle$, in suitable vibrational basis sets $\{\chi_{n\nu}(\mathbf{Q})\}$:

$$\chi_n^{(j)}(\mathbf{Q}) = \sum_\nu \alpha_{n\nu,j}|\chi_{n\nu}\rangle \quad (4)$$

The exact vibronic energies ε_j and the expansion coefficients $\alpha_{n\nu,j}$ are thereafter obtained by diagonalizing the vibronic Hamiltonian matrix. This matrix has the following elements:[22]

$$H_{m\mu,n\nu} = \langle\chi_{m\mu}|[\hat{T}_N(\mathbf{Q}) + E_n(\mathbf{Q}) + \hat{\Lambda}_{nn}(\mathbf{Q})]\delta_{mn} + (1 - \delta_{mn})\hat{\Lambda}_{mn}(\mathbf{Q})|\chi_{n\nu}\rangle \quad (5)$$

where the nonadiabatic coupling operator is defined by:

$$\hat{\Lambda}_{mn}(\mathbf{Q}) = -\frac{\hbar^2}{2}\sum_k\left[\int d^3\mathbf{r}\Phi_m^*(\mathbf{r},\mathbf{Q})\frac{\partial^2\Phi_n(\mathbf{r},\mathbf{Q})}{\partial Q_k^2} + 2\int d^3\mathbf{r}\Phi_m^*(\mathbf{r},\mathbf{Q})\frac{\partial\Phi_n(\mathbf{r},\mathbf{Q})}{\partial Q_k}\frac{\partial}{\partial Q_k}\right] \quad (6)$$

Equation 5 suggests that the adiabatic vibrational states $\chi_{n\nu}(\mathbf{Q})$ should be chosen as the solutions of the unperturbed equation:

$$[\hat{T}_N(\mathbf{Q}) + E_n(\mathbf{Q}) + \hat{\Lambda}_{nn}(\mathbf{Q})]|\chi_{n\nu}\rangle = \varepsilon_{n\nu}^0|\chi_{n\nu}\rangle \quad (7)$$

where $\varepsilon_{n\nu}{}^0$ are defined as the zero-order adiabatic vibronic energy levels. By this choice for the vibrational basis sets, the Hamiltonian matrix elements take the following form:

$$H_{m\mu,n\nu} = \varepsilon_{n\nu}^0\delta_{mn}\delta_{\mu\nu} + (1 - \delta_{mn})\langle\chi_{m\mu}|\hat{\Lambda}_{mn}(\mathbf{Q})|\chi_{n\nu}\rangle \quad (8)$$

where the matrix elements $\langle\chi_{m\mu}|\hat{\Lambda}_{mn}(\mathbf{Q})|\chi_{n\nu}\rangle$ are the vibrational overlap integrals modulated by the nonadiabatic operator. The choice of vibrational basis sets is, in principle, free. To avoid the evaluation of the modulated vibrational overlap integrals, the other choice for the vibrational basis sets is to employ the vibrational states of a particular electronic state, for example, of the ground electronic state, to expand the expansion coefficients of each electronic state. In this case, although the evaluation of the vibrational overlap integrals is avoided, the unperturbed vibronic Hamiltonian matrix is no longer diagonal.

In the diabatic electronic representation, the diabatic electronic states $\{\phi_n(\mathbf{r},\mathbf{Q})\}$ are defined as a unitary transformation of the adiabatic electronic states such that the electronic states become smoothly varying functions of the nuclear coordinates and the derivative coupling are sufficiently small to be neglected.[33] The exact vibronic states are then expanded as:

$$|\psi_j\rangle = \sum_n \tilde{\chi}_n^{(j)}(\mathbf{Q})|\phi_n\rangle = \sum_{n\nu}\tilde{\alpha}_{n\nu,j}|\phi_n\tilde{\chi}_{n\nu}\rangle \quad (9)$$

where $\{\tilde{\chi}_{n\nu}(\mathbf{Q})\}$ is a suitable vibrational basis set. As in the adiabatic case, the exact vibronic energies ε_j and the expansion coefficients $\tilde{\alpha}_{n\nu,j}$ are determined by diagonalizing the vibronic Hamiltonian matrix, which has the following matrix elements:

$$\tilde{H}_{m\mu,n\nu} = \langle\tilde{\chi}_{m\mu}|[\hat{T}_N(\mathbf{Q}) + \tilde{E}_n(\mathbf{Q})]\delta_{mn} + (1 - \delta_{mn})\tilde{\Lambda}_{mn}(\mathbf{Q})|\tilde{\chi}_{n\nu}\rangle \quad (10)$$

where $\tilde{E}_n(\mathbf{Q}) = \tilde{\Lambda}_{nn}(\mathbf{Q})$ and the diabatic coupling elements are defined by:

$$\tilde{\Lambda}_{mn}(\mathbf{Q}) = \int d^3\mathbf{r}\phi_m^*(\mathbf{r},\mathbf{Q})[\hat{T}_e(\mathbf{r}) + \hat{U}(\mathbf{r},\mathbf{Q})]\phi_n(\mathbf{r},\mathbf{Q}) \quad (11)$$

Again, eq 10 recommends that the diabatic vibrational states $\{\tilde{\chi}_{n\nu}(\mathbf{Q})\}$ should be chosen as the solutions of the unperturbed equation:

$$[\hat{T}_N(\mathbf{Q}) + \tilde{E}_n(\mathbf{Q})]|\tilde{\chi}_{n\nu}\rangle = \tilde{\varepsilon}_{n\nu}^0|\tilde{\chi}_{n\nu}\rangle \quad (12)$$

where $\tilde{\varepsilon}_{n\nu}^\phi$ are defined as the zero-order diabatic vibronic energy levels. By this choice, the vibronic Hamiltonian matrix reduces to:

$$\tilde{H}_{m\mu,n\nu} = \tilde{\varepsilon}_{n\nu}^0\delta_{mn}\delta_{\mu\nu} + (1 - \delta_{mn})\langle\tilde{\chi}_{m\mu}|\tilde{\Lambda}_{mn}(\mathbf{Q})|\tilde{\chi}_{n\nu}\rangle \quad (13)$$

It is seen that neither the adiabatic nor the diabatic vibronic states are the true eigenstates of the vibronic Hamiltonian, so they are not the stationary states, and the off-diagonal elements of the vibronic Hamiltonian matrix induce transitions between the adiabatic or the diabatic vibronic states. Indeed, the general solution of the time-dependent Schrodinger equation may be written as:

$$|\psi(t)\rangle = \sum_j c_j\exp(-i\varepsilon_j t/\hbar)|\psi_j\rangle \quad (14)$$

Let us consider the adiabatic expansion, eqs 2 and 4, for our discussion (similar argument applies to the diabatic expansion, eq 9). To find the constants c_1, c_2,..., we need some initial conditions. Suppose the system is prepared in the adiabatic vibronic state $|\Phi_s\chi_{s\sigma}\rangle$ at time $t = 0$, we then simply find $c_j = \alpha_{s\sigma,j}^*$ noticing that the matrix $\alpha_{n\nu,j}$ is unitary. Therefore, the probability amplitude $a_{s\sigma}(t)$ that the system at time t is still in the state $|\Phi_s\chi_{s\sigma}\rangle$ is given by:

$$a_{s\sigma}(t) = \sum_j |\alpha_{s\sigma,j}|^2\exp(-i\varepsilon_j t/\hbar) \quad (15)$$

and the probability amplitude $a_{l\lambda}(t)$ of finding the system at time t in the state $|\Phi_l\chi_{l\lambda}\rangle$, assuming it was initially prepared in the state $|\Phi_s\chi_{s\sigma}\rangle$, by:

$$a_{l\lambda}(t) = \sum_j \alpha_{s\sigma,j}^*\alpha_{l\lambda,j}\exp(-i\varepsilon_j t/\hbar) \quad (16)$$

For the case in which a vibronic state $|\Phi_s\chi_{s\sigma}\rangle$, at an energy $\varepsilon_{s\sigma}^0$, is embedded in a dense manifold of the high vibrational levels of a second adiabatic electronic state, an approximate expression for the probability amplitude $a_{s\sigma}(t)$ is given by:[22]

$$a_{s\sigma}(t) \simeq \exp\left[-\frac{i}{\hbar}(\varepsilon_{s\sigma}^0 + \Delta\varepsilon_{s\sigma}) - \frac{1}{2}\Gamma_{s\sigma}t\right] \quad (17)$$

where $\Delta\varepsilon_{s\sigma}$ is the shift of the zero-order adiabatic vibronic energy level $\varepsilon_{s\sigma}^0$, due to the off-diagonal vibronic matrix elements $H_{l\lambda,s\sigma}$ in second-order, and the decay rate constant $\Gamma_{s\sigma}$ is defined as:

$$\Gamma_{s\sigma} = \frac{2\pi}{\hbar}\sum_\lambda |H_{l\lambda,s\sigma}|^2\delta(\varepsilon_{s\sigma}^0 - \varepsilon_{l\lambda}^0) \quad (18)$$

2.2. Diabatic and Adiabatic Potential Energy Surfaces. The diabatic potential energy surfaces $\tilde{E}_m(\mathbf{Q})$ are defined as the diagonal elements of the electronic Hamiltonian matrix in diabatic electronic states.The diabatic potential surfaces are, by assumption, the slowly varying function of vibrational normal coordinates $\mathbf{Q}$. Thus, we may expand $\tilde{E}_m(\mathbf{Q})$ of any electronic state about a reference nuclear configuration (say, the equilibrium configuration of the ground electronic state of the molecule):

$$\tilde{E}_m(\mathbf{Q}) = \tilde{E}_m(\mathbf{0''}) + \sum_k \kappa_k^{(m)} Q''_k + \frac{1}{2}\sum_{kl} \eta_{kl}^{(m)} Q''_k Q''_l = \tilde{E}_m(\mathbf{0''}) + \mathbf{Q''}^T \boldsymbol{\kappa}^{(m)} + \frac{1}{2}\mathbf{Q''}^T \boldsymbol{\eta}^{(m)} \mathbf{Q''} \quad (19)$$

where $\tilde{E}_m(\mathbf{0''})$ is the vertical excitation energy, and $\kappa_k^{(m)}$ and $\eta_{kl}^{(m)}$ are the first and the second derivatives of $\tilde{E}_m(\mathbf{Q})$ evaluated at the ground electronic state equilibrium configuration. Notice that for the ground electronic state, that is, for $m = g$, the linear terms in eq 19 vanish and $\eta_{kl}^{(g)} = \Omega''^2_k \delta_{kl}$, where $\{\Omega''_k\}$ are the set of the diabatic angular vibrational frequencies of the ground electronic state, which are equal to the adiabatic vibrational angular frequencies in the absence of vibronic coupling.

To evaluate the vibronic Hamiltonian matrix elements given by eq 10, in which the vibrational basis sets belong to different electronic states, first we need to carry out a transformation on eq 19 to change the vibrational variables to those of the corresponding electronic states. To that end, we may employ the orthogonal transformation (the so-called Duschinsky transformation[27]):

$$\mathbf{Q'} = \mathbf{J}^{(m)} \mathbf{Q''} + \mathbf{D}^{(m)} \quad (20)$$

where $\mathbf{J}^{(m)}$ is the Duschinsky rotation matrix and $\mathbf{D}^{(m)}$ is the displacement vector whose components are the shift of the equilibrium configuration of the excited electronic state with respect to the ground electronic state equilibrium configuration. The matrix $\mathbf{J}^{(m)}$ is chosen to diagonalize the matrix $\boldsymbol{\eta}^{(m)}$:

$$\mathbf{J}^{(m)} \boldsymbol{\eta}^{(m)} \mathbf{J}^{(m)T} = \boldsymbol{\Lambda'} = \mathrm{diag}(\Omega'^2_1, \Omega'^2_2, ..., \Omega'^2_N) \quad (21)$$

where $\{\Omega'_k\}$ are the set of the diabatic angular vibrational frequencies corresponding to the diabatic electronic state $|\phi_m\rangle$, and the matrix $\mathbf{D}^{(m)}$ to remove the linear terms from eq 19:

$$\mathbf{D}^{(m)} = \boldsymbol{\Lambda'}^{-1} \mathbf{J}^{(m)} \boldsymbol{\kappa}^{(m)} = \mathbf{J}^{(m)} \boldsymbol{\eta}^{-(m)} \boldsymbol{\kappa}^{(m)} \quad (22)$$

where $\boldsymbol{\eta}^{-(m)}$ is the inverse of the matrix $\boldsymbol{\eta}^{(m)}$. So, we obtain:

$$\tilde{E}_m(\mathbf{Q}) = \tilde{E}_m(\mathbf{0'}) + \frac{1}{2}\mathbf{Q'}^T \boldsymbol{\Lambda'} \mathbf{Q'} \quad (23)$$

where $\tilde{E}_m(\mathbf{0'})$ is the "bottom of the well" energy of the mth electronic state:

$$\tilde{E}_m(\mathbf{0'}) = \tilde{E}_{\mathrm{m}}(\mathbf{0''}) - \frac{1}{2}\mathbf{D}^{(m)T} \boldsymbol{\Lambda'} \mathbf{D}^{(m)} \quad (24)$$

A similar transformation may be applied for any excited electronic state. By these transformations, the basis sets $\{\tilde{\chi}_{m\mu}(\mathbf{Q})\}$ become the harmonic oscillator wave functions centered on the corresponding diabatic potential energy surface.

The adiabatic potential energy surfaces are the eigenvalues of the electronic Hamiltonian matrix in the diabatic electronic states. When two electronic states, say m and n, are close to each other and well separated from the rest, the diagonalization of the electronic Hamiltonian matrix is the easiest and leads to the adiabatic potential energy surfaces as well as the diabatic-to-adiabatic transformation matrix. The adiabatic potential energy surfaces are as follows:

$$E_m(\mathbf{Q}), E_n(\mathbf{Q}) = \frac{1}{2}[\tilde{E}_n(\mathbf{Q}) + \tilde{E}_m(\mathbf{Q})] \pm \frac{1}{2}\{[\tilde{E}_n(\mathbf{Q}) - \tilde{E}_m(\mathbf{Q})]^2 + 4|\tilde{\Lambda}_{mn}(\mathbf{Q})|^2\}^{1/2} \quad (25)$$

where $\tilde{\Lambda}_{mn}(\mathbf{Q})$ are the off-diagonal matrix elements of the electronic Hamiltonian in the diabatic representation. Expanding the square-root term, we obtain:

$$E_m(\mathbf{Q}) = \tilde{E}_m(\mathbf{Q}) - \sum_{j=1}^{\infty} \binom{1/2}{j} 2^{2j-1} \frac{|\tilde{\Lambda}_{mn}(\mathbf{Q})|^{2j}}{[\tilde{E}_n(\mathbf{Q}) - \tilde{E}_m(\mathbf{Q})]^{2j-1}} \quad (26a)$$

and

$$E_n(\mathbf{Q}) = \tilde{E}_n(\mathbf{Q}) + \sum_{j=1}^{\infty} \binom{1/2}{j} 2^{2j-1} \frac{|\tilde{\Lambda}_{mn}(\mathbf{Q})|^{2j}}{[\tilde{E}_n(\mathbf{Q}) - \tilde{E}_m(\mathbf{Q})]^{2j-1}} \quad (26b)$$

where $\binom{1/2}{j}$ is the binomial coefficient.

Suppose that the diabatic electronic states $|\phi_n\rangle$ and $|\phi_m\rangle$ are linearly coupled by the nontotally symmetric vibrational modes that belong to irreducible representation, say Γ_p, and that we can assume the following up-to-second-order expansion for $\tilde{\Lambda}_{mn}(\mathbf{Q})$ in terms of the ground electronic state vibrational modes:

$$\tilde{\Lambda}_{mn}(\mathbf{Q}) = \sum_p \lambda_p Q''_p + \sum_{i,j} c_{ij} Q''_i Q''_j \quad (27)$$

where λ_p and c_{ij} are the first-and second order interstate coupling constants, respectively. The first sum goes over all modes belonging to Γ_p and the second sum over all pairs of modes, the product of which belongs to Γ_p.

We can now express the adiabatic potential surfaces in terms of vibrational variables of the corresponding excited electronic state. Using eq 19 (and the similar expression for $\tilde{E}_n(\mathbf{Q})$) along with eq 20, the energy difference in the denominator of eq 26a can be written as:

$$\tilde{E}_n(\mathbf{Q}) - \tilde{E}_m(\mathbf{Q}) = G^{(m)} + \mathbf{g}^{(m)T} \mathbf{Q'} + \frac{1}{2}\mathbf{Q'}^T \mathbf{J}^{(m)} (\boldsymbol{\eta}^{(n)} - \boldsymbol{\eta}^{(m)}) \mathbf{J}^{(m)T} \mathbf{Q'} \quad (28)$$

where

$$G^{(m)} = 2\Delta - (\boldsymbol{\kappa}^{(n)} - \boldsymbol{\kappa}^{(m)})^T (\boldsymbol{\eta}^{-(m)} \boldsymbol{\kappa}^{(m)}) + \frac{1}{2}(\boldsymbol{\eta}^{-(m)} \boldsymbol{\kappa}^{(m)})^T (\boldsymbol{\eta}^{(n)} - \boldsymbol{\eta}^{(m)}) (\boldsymbol{\eta}^{-(m)} \boldsymbol{\kappa}^{(m)}) \quad (29a)$$

and the column matrix $\mathbf{g}^{(m)}$ is defined by:

$$\mathbf{g}^{(m)} = \mathbf{J}^{(m)} [(\boldsymbol{\kappa}^{(n)} - \boldsymbol{\kappa}^{(m)}) - (\boldsymbol{\eta}^{(n)} - \boldsymbol{\eta}^{(m)}) (\boldsymbol{\eta}^{-(m)} \boldsymbol{\kappa}^{(m)})] \quad (29b)$$

Here, $\tilde{E}_n(\mathbf{0''}) - \tilde{E}_m(\mathbf{0''}) = 2\Delta$ is the vertical energy gap between the electronic states m and n.

Substituting eqs 27 and 28 into eq 26a and making use of eq 20, we obtain the following expression for the adiabatic potential surface of the electronic state m in $\mathbf{Q'}$-space:

$$E_m(\mathbf{Q'}) = \tilde{E}_m(\mathbf{0'}) + \frac{1}{2}\mathbf{Q'}^T \boldsymbol{\Lambda'} \mathbf{Q'} - \sum_{l=1}^{\infty} \binom{1/2}{l} \left(\frac{2}{G^{(m)}}\right)^{2l-1} \times \left\{ \sum_p \left(\lambda_p - \sum_j c_{pj} (\boldsymbol{\eta}^{-(m)} \boldsymbol{\kappa}^{(m)})_j \right) (\mathbf{J}^{(m)T} \mathbf{Q'})_p + \sum_{i,j} c_{ij} (\mathbf{J}^{(m)T} \mathbf{Q'})_i (\mathbf{J}^{(m)T} \mathbf{Q'})_j \right\}^{2l} \times \left[1 + \frac{1}{G^{(m)}} \mathbf{g}^{(m)T} \mathbf{Q'} + \frac{1}{2G^{(m)}} \mathbf{Q'}^T \mathbf{J}^{(m)} (\boldsymbol{\eta}^{(n)} - \boldsymbol{\eta}^{(m)}) \mathbf{J}^{(m)T} \mathbf{Q'}\right]^{-(2l-1)} \quad (30)$$

The second term in the brace and the third term in the bracket of eq 30 are small and may be ignored, and thereafter the adiabatic potential energy takes more tractable form. The

adiabatic angular vibrational frequencies of the modes belonging to Γ_p can be directly read from eq 30:

$$\omega'^2_k = \Omega'^2_k - \frac{2}{G^{(m)}}\sum_{pp'} J^{(m)}_{kp} J^{(m)}_{kp'}\left(\lambda_p - \sum_j c_{pj}(\boldsymbol{\eta}^{-(m)}\boldsymbol{\kappa}^{(m)})_j\right)\times \left(\lambda_{p'} - \sum_j c_{p'j}(\boldsymbol{\eta}^{-(m)}\boldsymbol{\kappa}^{(m)})_j\right) \quad (31)$$

where $k = 1, 2, ..., n$, noticing that the remaining modes, those do not participate in the coupling, have the same adiabatic and diabatic frequencies. Also, it must true that for $k \neq l$:

$$\sum_{pp'} J^{(m)}_{kp} J^{(m)}_{lp'}\left(\lambda_p - \sum_j c_{pj}(\boldsymbol{\eta}^{-(m)}\boldsymbol{\kappa}^{(m)})_j\right)\times \left(\lambda_{p'} - \sum_j c_{p'j}(\boldsymbol{\eta}^{-(m)}\boldsymbol{\kappa}^{(m)})_j\right) = 0 \quad (32)$$

For a single inducing mode, eq 31 reduces to:

$$\omega'^2_p = \Omega'^2_p - \frac{2}{G^{(m)}}\left(\lambda_p - \sum_j c_{pj}(\boldsymbol{\eta}^{-(m)}\boldsymbol{\kappa}^{(m)})_j\right)^2 \quad (33)$$

and if the coupling is weak, we have $\omega'^2_p = \Omega'^2_p - \lambda_p{}^2/\Delta$.

The adiabatic potential surface $E_n(\mathbf{Q}')$ is obtained from $E_m(\mathbf{Q}')$ in eq 30 by changing the sign of the third term of eq 30 (minus to plus), replacing m by n everywhere except in the differences $(\boldsymbol{\kappa}^{(n)} - \boldsymbol{\kappa}^{(m)})$ and $(\boldsymbol{\eta}^{(n)} - \boldsymbol{\eta}^{(m)})$ wherever they appear, and noticing that $\mathbf{Q}'$ now refers to the electronic state n. Likewise, the adiabatic vibrational frequencies of Γ_p modes are obtained from eq 31 by changing the sign of the second term (minus to plus) and replacing m by n. Again, $(\boldsymbol{\kappa}^{(n)} - \boldsymbol{\kappa}^{(m)})$ and $(\boldsymbol{\eta}^{(n)} - \boldsymbol{\eta}^{(m)})$ differences remain unchanged.

2.3. Internal Conversion Decay Rate Constants. It has been shown that the thermally averaged internal conversion decay rate constant $k_{IC}(\Omega_{ab},T)$ from the statistically equilibrated initial vibronic states $\{|a\alpha\rangle\}$ to the manifold of the final states $\{|b\beta\rangle\}$ may be expressed as the Fourier transform of the time domain generating function $G(t)$:[28−30]

$$k_{IC}(\Omega_{ab}, T) = \sum_\alpha \rho_\alpha(T)\Gamma_{a\alpha} = \int_{-\infty}^{\infty} dt\, \exp(i\Omega_{ab}t)G(t) \quad (34)$$

where generating function is defined by:

$$G(t) = \frac{1}{\hbar^2}\sum_\alpha \sum_\beta \rho_\alpha(T)|H_{a\alpha,b\beta}|^2\exp[i(E_\alpha - E_\beta)t/\hbar] \quad (35)$$

Here, $\rho_\alpha(T)$ is the Boltzmann distribution function for the initial vibronic states, Ω_{ab} is the zero−zero transition frequency, E_α and E_β are the (harmonic) vibrational energies (excluding the zero-point energies) of the electronic states a and b, respectively, and $H_{a\alpha,b\beta}$ are the dynamic off-diagonal elements of the Hamiltonian matrix (in the adiabatic, eq 8, or the diabatic, eq 13, electronic representation) that induce the internal conversion transitions between the electronic states a and b.

In our previous work,[22] we derived general expressions for the generating function for two cases: the case in which the internal conversion takes place between two adiabatic, and the case in which it takes place between two diabatic harmonic potential surfaces. The derivation included the effects of displacement−distortion−rotation of the harmonic potential surfaces, the promoting modes, and the temperature. In the following, we shall present the result obtained for these cases.

For the case in which internal conversion occurs between the adiabatic electronic states, the generating function has the following form:

$$G(t) = 2^N h(t)(\det \boldsymbol{\Gamma}'^{-1}\boldsymbol{\Gamma}''^{-1}\mathbf{T}'\mathbf{T}''\mathbf{W}_1\mathbf{W}_2)^{-1/2}\exp(-\mathbf{D}^T\mathbf{W}_3^{-1}\mathbf{D}) \quad (36)$$

with

$$h(t) = \frac{1}{2}\mathbf{R}^\dagger(-\mathbf{W}_3^{-1} + \mathbf{W}_4^{-1})\mathbf{R} + (\mathbf{R}^\dagger\mathbf{W}_3^{-1}\mathbf{D})(\mathbf{D}^T\mathbf{W}_3^{-1}\mathbf{R}) \quad (37)$$

where the $N \times N$ symmetric matrices $\mathbf{W}_1$,$\mathbf{W}_2$,$\mathbf{W}_3$, and $\mathbf{W}_4$ and the $N \times N$ diagonal matrices $\boldsymbol{\Gamma}'$, $\boldsymbol{\Gamma}''$, $\mathbf{T}'$, and $\mathbf{T}''$ are defined in ref 22, and $\mathbf{R}$ is the N-dimensional column vector of the nonadiabatic coupling matrix elements:

$$\{R_p = -i\hbar\langle\Phi_a|\partial/\partial Q'_p|\Phi_b\rangle_0, p = 1, 2, ..., N\}$$

$\langle...\rangle_0$ represents the value of the matrix elements in the vicinity of some reference nuclear configuration, say the equilibrium nuclear configuration of the ground electronic state, and $\mathbf{D}$ is the N-dimensional displacement vector whose components $\{D_j\}$ are the equilibrium shifts between two electronic states a and b. It should be noted that the "double primed" quantities refer to the lower and the "single primed" quantities refer to the upper electronic state. For the nontotally symmetric mode Q_j, $D_j = 0$, and for the accepting mode Q_j, $R_j = 0$.

For the internal conversion between the diabatic electronic states (belonging to different symmetry species), we obtain a similar expression for the generating function:

$$\tilde{G}(t) = 2^N\tilde{h}(t)(\det \boldsymbol{\Gamma}'^{-1}\boldsymbol{\Gamma}''^{-1}\mathbf{T}'\mathbf{T}''\mathbf{W}_1\mathbf{W}_2)^{-1/2}\exp(-\mathbf{D}^T\mathbf{W}_3^{-1}\mathbf{D}) \quad (38)$$

with

$$\tilde{h}(t) = \frac{1}{2}\tilde{\mathbf{R}}^\dagger\mathbf{J}(-\mathbf{W}_2^{-1} + \mathbf{W}_1^{-1})\mathbf{J}^T\tilde{\mathbf{R}} + (\tilde{\mathbf{R}}^\dagger\mathbf{J}\mathbf{W}_1^{-1}\boldsymbol{\Gamma}''\mathbf{A}''\mathbf{J}^T\mathbf{D})\times (\mathbf{D}^T\mathbf{J}\boldsymbol{\Gamma}''\mathbf{A}''\mathbf{W}_1^{-1}\mathbf{J}^T\tilde{\mathbf{R}}) \quad (39)$$

Here, $\tilde{R}_p = (1/\hbar)\sum_{p'}J^{(a)}_{pp'}\lambda_{p'}$, where $\mathbf{J}^{(a)}$ is the Duschinsky matrix between the excited a and the ground electronic states, and λ_p is the first-order interstate coupling constant defined in eq 27. All matrices ($\boldsymbol{\Gamma}'$,$\boldsymbol{\Gamma}''$,$\mathbf{T}'$,$\mathbf{T}''$,$\mathbf{A}'$,$\mathbf{A}''$,$\mathbf{W}_1$,$\mathbf{W}_2$,$\mathbf{W}_3$) have the same definitions as in the adiabatic case, except that the diabatic angular vibrational frequencies $\{\Omega'_k\}$ and $\{\Omega''_k\}$ have to be used in the related equations.

3. Results and Discussion

In this section, we shall apply the low-temperature limit versions of eqs 36 and 38 to calculate decay rate constants for the $^1B_{2u} \rightarrow {}^1B_{3u}$, $^1B_{2u} \rightarrow {}^1A_g$, and $^1B_{3u} \rightarrow {}^1A_g$ internal conversions in pyrazine. In the low temperature limit, the internal conversions take place from the ground vibrational level of the upper electronic state. The relative positions of three electronic states of interest are displayed in the following diagram.

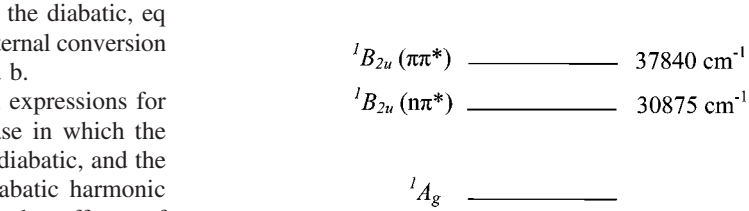

The method of saddle point is used for approximate evaluation of integral given in eq 34.[31,32] The method is based on the fact that the major contribution from the integrand in the integral $\int_{-\infty}^{\infty} dt\, \exp[f(t)]$ comes from the vicinity of the saddle point t_s where $f(t)$ is maximum [$f'(t_s) = 0$].

TABLE 1: Vibrational Frequencies (cm^{-1}) of ^1A_g, $^1B_{3u}$, and $^1B_{2u}$ Electronic States of Pyrazine[a]

vibration		^1A_g	$^1B_{3u}$ calc.		$^1B_{2u}$ calc.	
notation	irrep	obs.[b]	CASSCF	CIS	CASSCF	CIS
6a	a_g	596	608	595	542	593
1	a_g	1015	1012	1008	1037	1013
9a	a_g	1230	1199	1219	1250	1202
8a	a_g	1582	1497	1594	1644	1601
2	a_g	3055	3057	3056	3051	3057
6b	b_{3g}	704	650	619	620	659
3	b_{3g}	1346	1330	1818	1286	1755
8b	b_{3g}	1525	1022	757	1574	751
7b	b_{3g}	3040	3040	3014	2969	3037
12	b_{1u}	1021	477	477	895	941
18a	b_{1u}	1136	1045	1045	1077	1177
19a	b_{1u}	1484	1297	1297	1392	1424
13	b_{1u}	3012	2974	2974	2942	3017
18b	b_{2u}	1063	1040	1039	953	953
14	b_{2u}	1149	1432	1428	2031	2031
19b	b_{2u}	1416	1367	1495	1359	1359
20b	b_{2u}	3063	3069	3056	2991	2991
16a	a_u	341	345	423	190	190
17a	a_u	960	572	778	156	156
16b	b_{3u}	420	284	154	278	159
11	b_{3u}	785	707	813	653	745
4	b_{2g}	756	541	545	350	362
5	b_{2g}	983	884	823	674	972
10a	b_{1g}	919	769	820	769	820
			459 (427)	467 (491)	1313 (1559)	1648 (1450)

[a] In parentheses are the adiabatic vibrational frequencies of the mode b_{1g} at CASSCF/MRCI or CIS/MRCI level. [b] Reference 16.

Before proceeding with our theoretical results, we may outline some experimental observations that have been made on the decay rates of pyrazine.

Pyrazine exhibits a weak fluorescence both in solution[6] and in vapor,[7] but strong phosphorescence in vapor and condensed phases.[8,9] Yamazaki et al.[19] measured quantum yields for fluorescence and intersystem crossing and also fluorescence lifetimes in the vapor phase as a function of excitation energy, ranging from the ground vibrational level of $^1B_{3u}$ state to higher vibronic levels of $^1B_{2u}$ state. (For excitation at the electronic origin of the $^1B_{3u}-^1A_g$, the decay times $\tau_F \simeq 118$ ps, $\tau_{ISC} \simeq 119$ ps, and $\tau_{IC} \simeq 10$ ns were obtained.) They concluded that as excitation energy is increased, k_{ISC} remains almost constant throughout the energy region of $^1B_{3u}-^1A_g$ and $^1B_{2u}-^1A_g$ transitions, and that as the excitation energy exceeds 35 000 cm^{-1}, nonradiative decay rate increases rapidly with the excitation energy and for highly excited vibrational levels of $^1B_{3u}$ state it reaches as high as 4×10^{10} s^{-1} ($\tau_{IC} \simeq 25$ ps). They also estimated $k_{IC} \simeq 7.7 \times 10^{10}$ s^{-1} ($\tau_{IC} \simeq 13$ ps) for excitation at the electronic origin of the $^1B_{2u}-^1A_g$ followed by internal conversion to ^1A_g state (refer to Figure 5 of ref 19). In another experimental work, Wang et al.[20] excited pyrazine to within the vicinity of the zero vibrational level in $^1B_{2u}$ state and observed a decay time of (22 ± 1) ps, which was ascribed to $^1B_{3u} \rightarrow ^1A_g$ internal conversion after ultrafast dephasing from $^1B_{2u}$ state. The observed decay time was in agreement with the lifetime, 25 ps, of the higher vibronic level of $^1B_{3u}$ measured by Yamazaki et al. In addition, they measured a decay time (108 ± 2) ps after excitation to the zero-vibrational level of $^1B_{3u}$ state, which was ascribed to the growth of triplet states due to dephasing from optically prepared $^1B_{3u}$ pyrazine. Finally, in a more recent work, Stert et al.[21] measured a decay time of (20 ± 10) fs due to internal conversion from the ground vibrational level of $^1B_{2u}$ state, and an internal conversion decay time of (22 ± 1) ps for $^1B_{3u}$ state populated by the internal conversion from the $^1B_{2u}$ state.

We now go on with the theoretical results. The 24 vibrational modes of pyrazine molecule are distributed among the irreducible representations of the D_{2h} point group as:

$$5a_g + 4b_{3g} + 4b_{1u} + 4b_{2u} + 2a_u + 2b_{3u} + 2b_{2g} + b_{1g}$$

yz is the molecular plane with the z axis passing through the nitrogen atoms. The experimental ground-state vibrational frequencies of these modes are collected in Table 1.

The most comprehensive ab initio calculations of $^1B_{2u}$ and $^1B_{3u}$ diabatic potential energy surfaces to date have been made by Stock et al.[11] based on CASSCF (complete active space self-consistent field) and MRCI (multireference configuration interaction) and then by Raab et al.[16] based on CIS (single-excitation configuration interaction) ab initio calculations. The levels of calculations for the various coupling constants are as follows: The linear intrastate coupling constants $\kappa_j^{(m)}$ and $\kappa_j^{(n)}$ (for the five totally symmetric modes), where m and n refer to $^1B_{3u}$ and $^1B_{2u}$ electronic states, respectively, at the CASSCF, MRCI, and CIS levels; the quadratic intrastate coupling constants $\eta_{ij}^{(m)}$ and $\eta_{ij}^{(n)}$ at the CASSCF and CIS levels; the linear interstate coupling constant λ_p at the CASSCF, MRCI, and CIS levels; and finally the quadratic interstate coupling constants c_{ij} only at the CIS level. Here, we adopt all four sets of data, that is, CASSCF, CASSCF/MRCI, CIS, and CIS/MRCI data, to calculate the decay rate constants. However, it should be mentioned that the quadratic intrastate coupling constants $\eta_{ij}^{(m)}(\eta_{ij}^{(n)})$ defined in the present work are related to $\gamma_{ij}^{(m)}(\gamma_{ij}^{(n)})$ of ref 11 or $a_{ij}^{(m)}(b_{ij}^{(n)})$ of ref 16 as:

TABLE 2: Normalized Duschinsky Matrices for the $^1B_{3u}-{}^1A_g$, $^1B_{2u}-{}^1A_g$, and $^1B_{2u}-{}^1B_{3u}$ Electronic States of Pyrazine at the CASSCF Level[a]

electronic states	a_g modes	$\nu 2$	$\nu 8a$	$\nu 9a$	$\nu 1$	$\nu 6a$
$^1B_{3u}-{}^1A_g$	$\nu 2$	−0.9998 (0.9997)	−0.0165 (−0.0080)	0.0098 (−0.0192)	−0.0008 (−0.0058)	0.0006 (−0.0068)
	$\nu 8a$	−0.0155 (−0.0115)	0.9953 (−0.9815)	0.0928 (−0.1885)	−0.0143 (−0.0307)	0.0203 (0.0121)
	$\nu 9a$	−0.0113 (0.0179)	0.0928 (−0.1914)	−0.9955 (0.9671)	−0.0083 (0.1655)	−0.01018 (−0.0195)
	$\nu 1$	0.0011 (0.0027)	−0.0155 (0.0018)	0.0066 (−0.1678)	−0.9995 (0.9855)	0.0274 (0.0271)
	$\nu 6a$	0.0008 (0.0073)	−0.0188 (0.0080)	−0.0122 (0.0256)	0.0276 (−0.0231)	0.9994 (0.9994)
$^1B_{2u}-{}^1A_g$	$\nu 2$	−1.0000 (0.9990)	0.0012 (−0.0377)	0.0019 (−0.0147)	−0.0030 (−0.0208)	−0.0019 (−0.0028)
	$\nu 8a$	0.0013 (−0.0409)	0.9995 (−0.9677)	0.0304 (−0.2450)	−0.0115 (−0.0405)	0.0023 (0.0180)
	$\nu 9a$	−0.0017 (0.0054)	0.0300 (−0.2468)	−0.9988 (0.9685)	−0.0336 (0.0267)	−0.0189 (−0.0171)
	$\nu 1$	0.0029 (0.0188)	−0.0126 (−0.0341)	0.0319 (−0.0372)	−0.9973 (0.9971)	0.0654 (−0.0533)
	$\nu 6a$	−0.0021 (0.0047)	−0.0009 (0.0113)	−0.0211 (0.0189)	0.0648 (0.0544)	0.9977 (0.9983)
$^1B_{2u}-{}^1B_{3u}$	$\nu 2$	0.9998 (0.9994)	0.0169 (0.0288)	0.0096 (0.0075)	0.0018 (−0.0155)	−0.0027 (0.0042)
	$\nu 8a$	−0.0175 (−0.0283)	0.9977 (0.9978)	0.0625 (−0.0595)	−0.0037 (−0.0001)	−0.0171 (0.0047)
	$\nu 9a$	−0.0086 (−0.0112)	−0.0627 (0.0586)	0.9976 (0.9888)	0.0260 (−0.1371)	−0.0082 (0.0052)
	$\nu 1$	−0.0016 (0.0143)	0.0059 (0.0091)	−0.0254 (0.1369)	0.9990 (0.9874)	0.0377 (−0.0774)
	$\nu 6a$	0.0024 (−0.0029)	0.0164 (−0.0044)	0.0102 (0.0058)	−0.0376 (0.0774)	0.9991 (0.9970)

electronic states	b_{3g} modes	$\nu 7b$	$\nu 8b$	$\nu 3$	$\nu 6b$
$^1B_{3u}-{}^1A_g$	$\nu 7b$	−0.9996 (−0.9998)	−0.0258 (0.0101)	−0.0147 (−0.0110)	0.0028 (−0.0144)
	$\nu 8b$	0.0289 (−0.0080)	−0.9091 (−0.9089)	−0.3943 (−0.3673)	−0.1314 (0.1971)
	$\nu 3$	−0.0034 (0.01503)	−0.3951 (0.3582)	0.9184 (−0.9300)	−0.0230 (−0.0809)
	$\nu 6b$	0.0066 (−0.0119)	−0.1297 (0.2132)	−0.0310 (−0.0030)	0.9916 (0.9769)
$^1B_{2u}-{}^1A_g$	$\nu 7b$	1.0000 (−0.9998)	−0.0036 (0.0154)	−0.0011 (0.0077)	0.0012 (0.0067)
	$\nu 8b$	−0.0036 (−0.0182)	−0.9998 (−0.9080)	−0.0174 (−0.2910)	0.0034 (−0.3009)
	$\nu 3$	0.0010 (−0.0026)	−0.0174 (0.2912)	0.9999 (−0.9556)	−0.0011 (0.0457)
	$\nu 6b$	−0.0011 (0.0014)	0.0034 (−0.3009)	0.0012 (−0.0461)	1.0000 (0.9525)
$^1B_{2u}-{}^1B_{3u}$	$\nu 7b$	−0.9994 (0.9996)	0.0324 (−0.0075)	−0.0030 (−0.0172)	0.0082 (0.0216)
	$\nu 8b$	0.0296 (0.0165)	0.9152 (0.8730)	0.3790 (−0.0305)	0.1336 (−0.4865)
	$\nu 3$	−0.0153 (0.0154)	−0.3782 (0.09536)	0.9251 (0.9893)	−0.0298 (0.1097)
	$\nu 6b$	0.0038 (−0.0176)	−0.1350 (0.4783)	−0.0232 (−0.1419)	0.9906 (0.8665)

electronic states	b_{1u} modes	$\nu 13$	$\nu 19a$	$\nu 18a$	$\nu 12$
$^1B_{3u}-{}^1A_g$	$\nu 13$	(0.9992)	(−0.0200)	(0.0338)	(−0.0101)
	$\nu 19a$	(0.0079)	(0.9491)	(0.3116)	(−0.0444)
	$\nu 18a$	(0.0365)	(0.3024)	(−0.9421)	(−0.1405)
	$\nu 12$	(0.0158)	(0.0854)	(−0.1195)	(0.9890)
$^1B_{2u}-{}^1A_g$	$\nu 13$	1.0000 (0.9999)	0.0025 (0.0167)	−0.0003 (−0.0018)	0.0090 (0.0011)
	$\nu 19a$	−0.0018 (−0.0165)	0.9898 (0.9977)	0.1229 (0.0650)	−0.0720 (−0.0119)
	$\nu 18a$	0.0044 (−0.0026)	0.0661 (0.0615)	−0.8442 (−0.9794)	−0.5320 (−0.1923)
	$\nu 12$	−0.0080 (−0.0018)	0.1261 (0.0241)	−0.5217 (−0.1912)	0.8437 (0.9813)
$^1B_{2u}-{}^1B_{3u}$	$\nu 13$	0.9990 (0.9986)	0.0098 (0.0231)	0.0362 (0.0430)	0.0249 (0.0185)
	$\nu 19a$	−0.0166 (−0.0340)	0.9809 (0.9676)	0.1936 (0.2415)	−0.0014 (0.0655)
	$\nu 18a$	−0.0200 (−0.0349)	−0.1766 (−0.2383)	0.8902 (0.9682)	−0.4195 (−0.0680)
	$\nu 12$	−0.0367 (−0.0187)	−0.0804 (−0.0803)	0.4108 (0.0494)	0.9074 (0.9954)

electronic states	b_{2u} modes	$\nu 20b$	$\nu 19b$	$\nu 14$	$\nu 18b$
$^1B_{3u}-{}^1A_g$	$\nu 20b$	0.9998 (−0.9994)	−0.0186 (−0.0294)	−0.0023 (0.0149)	−0.0047 (−0.0124)
	$\nu 19b$	−0.0189 (0.0312)	−0.9924 (−0.9794)	−0.1137 (0.1942)	−0.0427 (0.0453)
	$\nu 14$	0.0001 (−0.0090)	−0.1138 (−0.1945)	0.9935 (−0.9808)	−0.0011 (0.0062)
	$\nu 18b$	0.0039 (−0.0138)	−0.0426 (0.0453)	−0.0038 (−0.0026)	0.9991 (0.9989)
$^1B_{2u}-{}^1A_g$	$\nu 20b$	1.0000	−0.0039	0.0034	0.0047
	$\nu 19b$	0.0043	0.9158	−0.3825	0.1229
	$\nu 14$	0.0015	−0.3895	−0.9202	0.0384
	$\nu 18b$	−0.0053	−0.0984	0.0830	0.9917
$^1B_{2u}-{}^1B_{3u}$	$\nu 20b$	0.9998 (−0.9992)	−0.0156 (0.0359)	0.0040 (−0.0115)	0.0087 (−0.0093)
	$\nu 19b$	−0.0124 (−0.0385)	−0.8706 (−0.9655)	−0.4843 (0.1977)	0.0853 (0.1651)
	$\nu 14$	0.0106 (−0.0042)	0.4895 (0.2045)	−0.8700 (0.9786)	0.0584 (0.0230)
	$\nu 18b$	−0.0083 (−0.0029)	0.0460 (0.1573)	0.0926 (−0.05610)	0.9946 (0.9860)

electronic states	a_u modes	$\nu 17a$	$\nu 16a$
$^1B_{3u}-{}^1A_g$	$\nu 17a$	0.8433 (0.9998)	−0.5375 (0.0216)
	$\nu 16a$	0.5375 (−0.0216)	0.8433 (0.9998)
$^1B_{2u}-{}^1A_g$	$\nu 17a$	0.9989	−0.0468
	$\nu 16a$	0.0468	0.9989
$^1B_{2u}-{}^1B_{3u}$	$\nu 17a$	0.8675 (0.9977)	0.4974 (−0.0684)
	$\nu 16a$	−0.4974 (0.0684)	0.8675 (0.9977)

electronic states	b_{3u} modes	$\nu 11$	$\nu 16b$
$^1B_{3u}-{}^1A_g$	$\nu 11$	0.9926 (0.9959)	0.1217 (−0.0910)
	$\nu 16b$	−0.1217 (0.0910)	0.9926 (0.9959)
$^1B_{2u}-{}^1A_g$	$\nu 11$	0.9892 (0.9990)	0.1466 (−0.0457)
	$\nu 16b$	−0.1466 (0.0457)	0.9892 (0.9990)
$^1B_{2u}-{}^1B_{3u}$	$\nu 11$	0.9997 (0.9990)	0.0251 (0.0454)
	$\nu 16b$	−0.0251 (−0.0454)	0.9997 (0.9990)

electronic states	b_{2g} modes	$\nu 5$	$\nu 4$
$^1B_{3u}-{}^1A_g$	$\nu 5$	0.9952 (0.9998)	−0.0979 (−0.0179)
	$\nu 4$	0.0979 (0.0179)	0.9952 (0.9998)
$^1B_{2u}-{}^1A_g$	$\nu 5$	0.9552 (0.9875)	0.2958 (0.1577)
	$\nu 4$	−0.2958 (−0.1577)	0.9552 (0.9875)
$^1B_{2u}-{}^1B_{3u}$	$\nu 5$	0.9217 (0.9845)	0.3879 (0.1754)
	$\nu 4$	−0.3879 (−0.1754)	0.9217 (0.9845)

[a] In parentheses are the corresponding values at the CIS level.

$$\gamma_{ij}^{(m)} = a_{ij} = \frac{1}{2}\left(\frac{\hbar^2}{\Omega''_i \Omega''_j}\right)^{1/2} (\eta_{ij}^{(m)} - \Omega''^2_i \delta_{ij}) \qquad (40)$$

with a similar relation between $\gamma_{ij}^{(n)} = b_{ij}$ and $\eta_{ij}^{(n)}$, where $\{\Omega''_j\}$ are the ground-state angular vibrational frequencies.

As stated before, eq 21, the eigenvalues of the symmetric matrix $\eta_{ij}^{(m)}(\eta_{ij}^{(n)})$ give the square of the diabatic angular vibrational frequencies of the normal modes in $^1B_{3u}$ ($^1B_{2u}$) electronic state, and the matrix constructed from its orthonormal eigenvectors determines the extent of the Duschinsky rotation of the normal modes of excited $^1B_{3u}$ ($^1B_{2u}$) with respect to those of the ground ^1A_g electronic state.The diabatic vibrational frequencies of normal modes in $^1B_{3u}$ and $^1B_{2u}$ electronic states calculated by diagonalization of the matrix $\eta_{ij}^{(m)}(\eta_{ij}^{(n)})$ are presented in Table 1. However, it has to be noted that the CASSCF-calculated matrix $\eta_{ij}^{(m)}$ for b_{1u} modes and the CIS-calculated $\eta_{ij}^{(n)}$ for the b_{2u} modes lead to negative eigenvalues (imaginary vibrational frequencies); therefore, the replacements CIS↔CASSCF data have been made. Also, the CIS-calculated vibrational frequencies of a_u modes in $^1B_{2u}$ state have been replaced by the corresponding more reasonable CASSCF values. The Duschinsky matrices connecting the excited and the ground states normal modes of the same symmetry species are collected in Table 2. The only vibrational mode that has different diabatic and adiabatic excited vibrational frequencies is the coupling mode ν_{10a} (of symmetry b_{1g}) whose adiabatic excited-state frequency is calculated from eq 33, taking $2\Delta = 0.846$ eV. The results are reported at the bottom of Table 1. The Duschinsky matrix **J** and the displacement vector **D** between the normal modes of two excited electronic states $^1B_{3u}$ and $^1B_{2u}$ can be calculated from the following relations:

$$\mathbf{J} = \mathbf{J}^{(n)}\mathbf{J}^{(m)T}, \mathbf{D} = \mathbf{D}^{(n)} - \mathbf{J}^{(n)}\mathbf{J}^{(m)T}\mathbf{D}^{(m)} \qquad (41)$$

Table 3 displays the Haung−Rhys factors corresponding to displacements $\mathbf{D}^{(m)}$, $\mathbf{D}^{(n)}$, and **D** (e.g., $S_j^{(m)} = \Omega''_j(D_j^{(m)})^2/2\hbar$) for the five totally symmetric modes.

Armed with Tables 1, 2, and 3, we can now calculate the decay time constants. Tables 4 displays the calculated decay time constants $\tau_{IC} = 1/k_{IC}$ for the $^1B_{2u}\rightarrow{}^1B_{3u}$ internal conversion. To explore the vibrational modes that have the highest contributions in the process, the decay time constants have been calculated for 2-mode (ν_{10a}, ν_{6a}), 3-mode (ν_{10a}, ν_{6a}, ν_1), 4-mode (ν_{10a}, ν_{6a}, ν_1, ν_{9a}), 6-mode (ν_{10a} plus all totally symmetric modes), 12-mode (all g-type symmetry modes), and 24-mode models; and to investigate the effects of distortions and rotations separately, each model is subdivided to displaced, displaced−distorted, and displaced−distorted−rotated submodels. For displaced submodels, the geometric averages of the vibrational frequencies Ω'_j and Ω''_j, that is, $(\Omega'_j\Omega''_j)^{1/2}$, are used. As Table 4 shows, the inclusion of more modes, beyond the four modes ν_{10a}, ν_{6a}, ν_1, ν_{9a}, does not have a drastic effect on the decay time constants. Besides, the distortions and rotations, as compared to the

TABLE 3: Haung−Rhys Factors S_j for the $^1B_{3u}-{}^1A_g$, $^1B_{2u}-{}^1A_g$, and $^1B_{2u}-{}^1B_{3u}$ Electronic States of Pyrazine

	$^1B_{3u}-{}^1A_g$		$^1B_{2u}-{}^1A_g$		$^1B_{2u}-{}^1B_{3u}$	
	CASSCF(CASSCF/MRCI)	CIS(CIS/MRCI)	CASSCF(CASSCF/MRCI)	CIS(CIS/MRCI)	CASSCF(CASSCF/MRCI)	CIS(CIS/MRCI)
S_2	0.003 (0.004)	0.002 (0.004)	0.004 (0.002)	0.001 (0.002)	0.0001 (0.001)	0.0007(0.002)
S_{8a}	0.015 (0.041)	0.005 (0.015)	0.009 (0.016)	0.004 (0.017)	0.000 (0.131)	0.006 (0.038)
S_{9a}	0.519 (0.650)	0.465 (0.591)	0.040 (0.037)	0.016 (0.022)	0.251 (0.337)	0.375 (0.457)
S_1	0.203 (0.072)	0.200 (0.196)	1.527 (1.252)	1.006 (1.381)	0.662 (0.771)	0.542 (0.850)
S_{6a}	0.840 (0.824)	0.771 (0.737)	0.900 (1.347)	1.447 (1.066)	3.539 (4.339)	4.420 (3.655)

TABLE 4: Zero−Zero Transition frequency, First-Order Vibronic Coupling Constant, and Decay Time Constant Associated with $^1B_{2u}\rightarrow{}^1B_{3u}$ Internal Conversion in Pyrazine

				other theoretical estimates	
$^1B_{2u}\rightarrow{}^1B_{3u}$	CASSCF(CASSCF/MRCI)	CIS(CIS/MRCI)	obs.	CASSCF	CIS
Ω_{ab} (cm^{-1})			6965[a]		
λ_{10a} (eV)	0.1676(0.1825)	0.208(0.1825)			
$\tau_{IC} = 1/k_{IC}$(fs):			(20 ± 10)[b]		
2-mode model					
displaced	567.8 (114.9)	46.2 (206.1)			
displaced−distorted	126.6 (36.9)	45.3 (200.8)			
3-mode model					
displaced	47.5 (16.7)	14.1 (20.6)		25[f]	
displaced−distorted	28.2 (11.2)	14.1 (20.6)			
4-mode model					
displaced	25.3 (9.8)	7.8 (10.0)			
displaced−distorted	18.0 (7.7)	7.8 (9.9)		30,[c] 40[d]	35[e]
6-mode model					
displaced	25.3 (8.1)	7.7 (9.4)			
displaced−distorted	17.9 (6.7)	7.7 (9.3)			
displaced−distorted−rotated	20.2 (6.9)	6.0 (7.1)			
12-mode model					
displaced	25.3 (8.1)	7.7 (9.4)			
displaced−distorted	16.1 (6.4)	7.5 (9.1)			
displaced−distorted−rotated	17.3 (6.5)	5.8 (6.1)			35[e]
24-mode model					
displaced	25.3 (8.1)	7.7 (9.4)			
displaced−distorted	11.1 (5.4)	5.5 (6.7)			
displaced−distorted−rotated	11.6 (5.5)	4.7 (5.7)			35[e]

[a] Reference 19. [b] Reference 21. [c] Reference 35. [d] Reference 24. [e] References 14 and 17. [f] References 23 and 24 (here, the parameters are estimated empirically; see the text).

TABLE 5: Zero−Zero Transition Frequency, Nonadiabatic Coupling Constant, and Decay Time Constant Associated with $^1B_{2u}\rightarrow{}^1A_g$ Internal Conversion in Pyrazine

$^1B_{2u}\rightarrow{}^1A_g$	CASSCF(CASSCF/MRCI)	CIS(CIS/MRCI)	obs.	types of modes
Ω_{ab} (cm^{-1})			37 840[a]	
$\langle\Phi_a\vert(\partial/\partial Q'_p)\vert\Phi_b\rangle$ (dimensionless)	3.60 (3.60) (Q'_{20b})	3.26 (3.13) (Q'_{20b})		
$\tau_{IC} = 1/k_{IC}$ (ps):			13	
2-mode model				20b, 17a
distorted	36.6 (36.6)	44.8 (48.3)		
3-mode model				20b, 17a, 16a
distorted	36.1 (36.2)	44.2 (47.8)		
distorted−rotated	36.3 (36.3)	44.4 (48.0)		
4-mode model				20b, 17a, 16a, 6a
displaced−distorted	29.1 (26.2)	31.5 (37.1)		
displaced−distorted−rotated	29.3 (26.3)	31.6 (37.3)		
5-mode model				20b, 17a, 16a, 6a, 1
displaced−distorted	15.1 (15.3)	20.3 (20.4)		
displaced−distorted−rotated	15.1 (15.3)	20.2 (20.5)		
6-mode model				20b, 17a, 16a, 6a, 1, 9a
displaced−distorted	14.7 (15.0)	20.2 (20.1)		
displaced−distorted−rotated	14.8 (15.0)	20.2 (20.2)		
8-mode model				20b, 17a, 16a, all a_g modes
displaced−distorted	14.5 (14.7)	20.1 (19.8)		
displaced−distorted−rotated	15.5 (15.8)	18.7 (18.4)		
17-mode model				all u-type symmetry modes, all a_g modes
displaced−distorted	13.5 (13.7)	18.0 (17.8)		
displaced−distorted−rotated	14.4 (14.7)	16.9 (16.6)		
24-mode model				all modes
displaced−distorted	12.3 (12.2)	14.0 (14.1)		
displaced−distorted−rotated	13 (13)	13 (13)		

[a] Reference 19.

TABLE 6: Zero−Zero Transition Frequency, Nonadiabatic Coupling Constant, and Decay Time Constant Associated with $^1B_{3u}\rightarrow{}^1A_g$ Internal Conversion in Pyrazine

$^1B_{3u}\rightarrow{}^1A_g$	CIS(CIS/MRCI)	obs.	types of modes
Ω_{ab} (cm^{-1})		30 875[a]	
$\langle\Phi_a\vert(\partial/\partial Q'_p)\vert\Phi_b\rangle$ (dimensionless)	26.27 (23.49) (Q'_{11})		
$\tau_{IC} = 1/k_{IC}$ (ns):		15	
2-mode model			11, 8b
distorted	123.0 (153.9)		
3-mode model			11, 8b, 16b
distorted	107.9 (134.9)		
distorted−rotated	106.9 (133.7)		
4-mode model			11, 8b, 16b, 6a
displaced−distorted	50.2 (64.1)		
displaced−distorted−rotated	70.2 (89.5)		
5-mode model			11, 8b, 16b, 6a, 9a
displaced−distorted	35.9 (38.0)		
displaced−distorted−rotated	34.9 (37.0)		
6-mode model			11, 8b, 16b, 6a, 9a, 1
displaced−distorted	28.8 (30.6)		
displaced−distorted−rotated	28.5 (30.3)		
8-mode model			11, 8b, 16b, all a_g modes
displaced−distorted	28.0 (28.6)		
displaced−distorted−rotated	26.1 (25.4)		
14-mode model			all g-type symmetry modes, 11, 16b
displaced−distorted	20.2 (21.4)		
displaced−distorted−rotated	25.3 (25.3)		
24-mode model			all modes
displaced−distorted	13.1 (13.8)		
displaced−distorted−rotated	15 (15)		

[a] Reference 19.

displacements, of the vibrational modes have minor effects on the decay process. It is also seen from Table 4 that the decay time constants based on the CASSCF parameters are generally higher than the corresponding values calculated from the CIS data and that the CASSCF/MRCI and CIS/MRCI data yield roughly the same values for the corresponding time constants. However, the present results are in good agreement with the observed decay time constants[21] of (20 ± 10) fs and the time constants calculated by other theoretical methods.[14,17,24,34,35] In ref 24, the calculations are performed at CASSCF levels, cc-pVDZ basis set, taking $\lambda_{10a} = 0.2489$ eV; and in ref 17, the value of the coupling constant λ_{10a} is not reported. Presumably,

it is taken as 0.1825 eV as in a previous work, ref 24, from the same authors. Reference 34 makes use of a displaced 3-mode model composed of ν_{10a}, ν_{6a}, and ν_1 modes in which the absolute values of the linear intrastate coupling constants are determined empirically and their signs from INDO/S CI calculations. The empirical coupling constant λ_{10a} is estimated to be 0.262 eV.

From the symmetry point of view, the promoting modes that are capable to induce $^1B_{2u}\rightarrow{}^1A_g$ radiationless transitions are four b_{2u} modes, and those that could be active in $^1B_{3u}\rightarrow{}^1A_g$ internal conversion are the two b_{3u} modes. Because the values of the nonadiabatic vibronic matrix elements for these promoting modes were not available, we varied them, using the 24-mode model, to obtain the decay times about 15 ns for $^1B_{3u}\rightarrow{}^1A_g$ internal conversion, and about 13 ps for $^1B_{2u}\rightarrow{}^1A_g$ internal conversion, as estimated by Yamazaki et al.[19] The results are presented in Tables 5 and 6. Our calculations show that for the $^1B_{2u}\rightarrow{}^1A_g$ internal conversion only the mode Q_{20b} plays the main role, as the promoting mode, and the rest do not have noticeable effects. Likewise, for the $^1B_{3u}\rightarrow{}^1A_g$ internal conversion, only the mode Q_{11} is the most effective promoting mode, and the effect of the mode Q_{16b} is negligibly small and may be ignored.

Attempts have been also made to find the minimal model for the internal conversions both with respect to the number and types of modes and with respect to the displacements, distortions, and rotations of the modes that are involved in the processes. Table 5 shows that, based on the CASSCF data, the 5-mode model consisting of promoting mode ν_{20b} (b_{2u}) and four accepting modes: ν_{17a} (a_u) plus three totally symmetric modes, which have the highest Haung−Rhys coupling constants (Table 3), that is, ν_{6a}, ν_1, and ν_{9a}, is capable of almost generating the observed decay time for $^1B_{2u}\rightarrow{}^1A_g$ internal conversion. As compared to the CASSCF, the calculations based on the CIS data converge more slowly to the observed decay time. Accordingly, Table 6 summarizes the calculations that have been carried out on the basis of CIS data for the decay time constant of the $^1B_{3u}\rightarrow{}^1A_g$ internal conversion. Although the calculations converge slowly, it seems that the 6-mode model composed of the promoting mode ν_{11} (b_{3u}) and five accepting modes, ν_{16b} (b_{3u}), ν_{8b} (b_{3g}), and three totally symmetric modes ν_{6a}, ν_1, and ν_{9a}, can roughly produce the observed decay time constant for the $^1B_{3u}\rightarrow{}^1A_g$ internal conversion and can be considered as the minimal model for this process. The use of CASSCF data for the $^1B_{3u}\rightarrow{}^1A_g$ internal conversion yields the results that are inconsistent with the other levels of calculations, which are skipped in Table 6.

Finally, it should be pointed out that the present calculations ignore the anharmonicities of the excited potential surfaces caused by the Q_{10a} mode, although it acts as an accepting mode for the internal conversions from the excited electronic states to the ground electronic state.

4. Summary and Conclusion

In this Article, the general expressions we derived in our previous work[22] for calculating the internal conversion rate constants between two adiabatic, eqs 34 and 36, and between two diabatic, eqs 34 and 38, electronic states have been used to estimate the decay rate constants for $^1B_{2u}(\pi\pi^*)\rightarrow{}^1B_{3u}(n\pi^*)$, $^1B_{2u}(\pi\pi^*)\rightarrow{}^1A_g$, and $^1B_{3u}(n\pi^*)\rightarrow{}^1A_g$ internal conversions in pyrazine. To calculate the adiabatic harmonic vibrational frequencies, an expression in terms of the diabatic coupling constants and the parameters determining the diabatic harmonic potential energy surfaces is also derived, eq 31.

The decay time constants have been calculated by employing the available CASSCF and MRCI ab initio data of Stock et al.[11] and CIS ab initio data of Raab at al.[16] for the diabatic potential energy surfaces of $^1B_{2u}$ and $^1B_{3u}$ electronic states of pyrazine. The eigenvalues of the symmetric matrix of the diabatic intrastate coupling constants give the diabatic vibrational frequencies of the normal modes in the excited $^1B_{3u}$ ($^1B_{2u}$) electronic state, Table 1, and its eigenvectors determine the Duschinsky rotation between normal modes (of the same symmetry species) of the excited $^1B_{3u}$ ($^1B_{2u}$) and the ground electronic states, Table 2. The displacement vectors of five totally symmetric modes of pyrazine expressed in terms of Haung−Rhys factors are presented in Table 3.

The decay time constants obtained in the present work for the $^1B_{2u}\rightarrow{}^1B_{3u}$ internal conversion, Table 4, are in good agreement with the decay time of (20 ± 10) fs[21] obtained experimentally. The distortions and rotations of the normal modes have minor effects on the decay time of this internal conversion. It has been also explored that a 4-mode model composed of the promoting mode ν_{10a} (b_{1g}) and three totally symmetric modes ν_{6a}, ν_1, and ν_{9a}, as the accepting modes, can approximately produce the observed decay time constant for this process.

The lack of the nonadiabatic vibronic matrix elements between the $^1B_{3u}$ ($^1B_{2u}$) and the ground electronic states led us to estimate them from the decay times observed by Yamazaki et al.[19] for the $^1B_{3u}\rightarrow{}^1A_g$ and $^1B_{2u}\rightarrow{}^1A_g$ internal conversions in pyrazine, Tables 5 and 6. On the basis of the present ab initio data, it was also concluded that the mode Q_{20b} (of symmetry b_{2u}) and the mode Q_{11} (of symmetry b_{3u}) were the most important promoting modes for the $^1B_{2u}\rightarrow{}^1A_g$ and $^1B_{3u}\rightarrow{}^1A_g$ internal conversions, respectively. In addition, we found that a 5-mode model consisting of promoting $\nu_{20b}(b_{2u})$ and four accepting modes, $\nu_{17a}(a_u)$ plus three totally symmetric modes ν_{6a}, ν_1, and ν_{9a}; and a 6-mode model composed of the promoting mode $\nu_{11}(b_{3u})$ and five accepting modes, $\nu_{16b}(b_{3u})$, $\nu_{8b}(b_{3g})$, and three totally symmetric modes ν_{6a}, ν_1, and ν_{9a}, could be considered as the minimal models for the $^1B_{2u}\rightarrow{}^1A_g$ and $^1B_{3u}\rightarrow{}^1A_g$ internal conversions, respectively.

Noted Added after ASAP Publication. This article posted ASAP on February 11, 2009. Equation 7 has been revised. The correct version posted February 13, 2009.

References and Notes

(1) Ito, M.; Shimada, R.; Kuraishi, T.; Mizushima, W. *J. Chem. Phys.* **1957**, *26*, 1508.
(2) Suzuka, I.; Mikami, N.; Ito, M. *J. Mol. Spectrosc.* **1974**, *52*, 21.
(3) Zalewski, E. F.; McClure, D. S.; Narva, D. L. *J. Chem. Phys.* **1974**, *61*, 2964.
(4) Narva, D. L.; McClure, D. S. *Chem. Phys.* **1975**, *11*, 151.
(5) Udagawa, Y.; Ito, M.; Suzuka, I. *Chem. Phys.* **1980**, *46*, 237.
(6) Cohen, B. J.; Goodman, L. *J. Chem. Phys.* **1967**, *46*, 713.
(7) Logan, L. M.; Ross, I. G. *Acta Phys. Pol.* **1968**, *34*, 721.
(8) Goodman, L.; Kasha, M. *J. Mol. Spectrosc.* **1958**, *2*, 58.
(9) Marzzaco, C. J.; Zalewski, E. F. *J. Mol. Spectrosc.* **1972**, *43*, 239.
(10) Woywod, C.; Domcke, W.; Sobolewski, A. L.; Werner, H.-J. *J. Chem. Phys.* **1994**, *100*, 1400.
(11) Stock, G.; Woywod, C.; Domcke, W.; Swinney, T.; Hudson, B. S. *J. Chem. Phys.* **1995**, *103*, 6851.
(12) Krempl, S.; Winterstetter, M.; Plöhn, H.; Domcke, W. *J. Chem. Phys.* **1994**, *100*, 926.
(13) Krempl, S.; Winterstetter, M.; Domcke, W. *J. Chem. Phys.* **1995**, *102*, 6499.
(14) Puzari, P.; Swathi, R. S.; Sarkar, B.; Adhikari, S. *J. Chem. Phys.* **2005**, *123*, 134317.
(15) Gerdts, T.; Manthe, U. *Chem. Phys. Lett.* **1998**, *295*, 167.
(16) Raab, A.; Worth, G. A.; Meyer, H.-D.; Cederbaum, L. S. *J. Chem. Phys.* **1999**, *110*, 936.
(17) Puzari, P.; Sarkar, B.; Adhikari, S. *J. Chem. Phys.* **2006**, *125*, 194316.

(18) Knee, J. L.; Doany, F. E.; Zewail, A. H. *J. Chem. Phys.* **1985**, *82*, 1042.
(19) Yamazaki, I.; Murao, T.; Yamanaka, T.; Yoshihara, K. *Faraday Discuss. Soc.* **1983**, *75*, 395.
(20) Wang, L.; Kohguchi, H.; Suzuki, T. *Faraday Discuss.* **1999**, *113*, 37.
(21) Stert, V.; Farmanara, P.; Radloff, W. *J. Chem. Phys.* **2000**, *112*, 4460.
(22) Islampour, R.; Miralinaghi, M. *J. Phys. Chem. A* **2007**, *111*, 9454.
(23) Schneider, R.; Domcke, W. *Chem. Phys. Lett.* **1988**, *150*, 235.
(24) Borrelli, R.; Peluso, A. *J. Chem. Phys.* **2003**, *119*, 8437.
(25) Smith, F. T. *Phys. Rev.* **1969**, *179*, 111.
(26) Longuet-Higgins, H. C. *Adv. Spectrosc.* **1961**, *2*, 429.
(27) Duschinsky, F. *Acta Phisicochim. URSS* **1937**, *7*, 551.
(28) Kubo, R. *Phys. Rev.* **1952**, *86*, 929.
(29) Kubo, R.; Toyozawa, Y. *Prog. Theor. Phys.* **1955**, *13*, 160.
(30) Lin, S. H. *J. Chem. Phys.* **1966**, *44*, 3759.
(31) Islampour, R.; Alden, R. G.; Wu, G. Y. C.; Lin, S. H. *J. Phys. Chem.* **1993**, *97*, 6793.
(32) Cushing, J. T. *Applied Analytical Mathematics for Physical Scientists*; Wiley: New York, 1975.
(33) Domcke, W.; Stock, G. In *Advances in Chemical Physics*; Prigogine, I., Rice, S. A., Eds.; Wiley: New York, 1977; Vol. 100.
(34) Seel, M.; Domcke, W. *J. Chem. Phys.* **1991**, *95*, 7806.
(35) Stock, G.; Domcke, W. *J. Phys. Chem.* **1993**, *97*, 12466.

JP8072206